Int. J. Nanosci. Nanotechnol., Vol. 20, No. 1, March 2024, pp. 1-9
DOI: 10.22034/ijnn.2024.561073.2264

Bio-Synthesis, Characterization and Catalytic Potential of Nanoparticles for Dyes Removal

Abubakar Iqbal* and Rehana Saeed

Department of Chemistry, Faculty of Science, University of Karachi,
75270, Karachi, Pakistan

(*) Corresponding author: abubakariqbal2626@gmail.com
(Received: 28 August 2022 and Accepted: 16 November 2023)

Abstract

The kinetics of catalytic degradation of methyl violet using biosynthesized silver nanoparticles was studied spectrophotometrically. The biosynthesis process synthesized the silver nanoparticles using Azadirachta indica leaves extract and characterized by spectral techniques. Uv spectra showed the reduction of silver nitrate into silver nanoparticles. Atomic force microscopy analysis showed the configuration, morphology, and size of silver nanoparticles. It was observed silver nanoparticles are spherical and produced in high percentages. The kinetics of degradation of methyl violet with silver nanoparticles was analyzed by observing the change in absorbance with respect to time at 583nm as a function of pH, concentration of nanoparticle, catalyst, and temperature. The reaction follows pseudo-first-order kinetics depends on the concentration of nanoparticles and is independent of the concentration of methyl violet. The degradation process was found to be more favorable at low temperatures and in the basic medium at pH 11 The activation parameters are also evaluated.

Keywords: *Biosynthesis, Silver nanoparticles (AgNPs), Characterization, Catalytic degradation, Dye*.

1. INRODUCTION

Dyes are water-soluble dispersible organic colorants, having applications in various industries. Synthetic dyestuffs are used extensively in textile, paper, printing industries, and dye houses [1]. Dyes have a complex aromatic molecular structure, which makes them more stable and more difficult to biodegrade. The structure of the dye contains aryl rings, which contain a delocalized electron system responsible for the absorption of electromagnetic radiation by changing the wavelength, depending on the energy of electron clouds [2, 3]. The addition of auxo chrome and chromophore results in a much alteration of the absorption maximum of the compound. – The CH_3 or $-C_2H_5$ group alerts the color of dyes by altering the energy in the delocalized electrons [4-6].

The industry used dyes for coloring and finishing their product; tons of dyes were lost to effluents due to in effecting of their process and remain in the environment as a result of the high stability of dyes to light and temperature [7]. These dyes are well known for their intensity of color and their shades of red, blue, and green. The toxicity, carcinogenicity, and mutagenicity of some of these dyes to biota make these xenobiotics an environmental problem [8]. The photolysis and photochemistry investigation of triaryl methane showed that they did not undergo photofading in a solution containing mild reducing agents. The reduction and oxidation reaction of triphenylmethane dyes incorporated in polymers, fibers, and polyelectrolytes have been studied to understand the photodegradation of this class of dyes[9, 10]. They are used in electrical devices, optical devices, biotechnology, textile industry, cosmetic industry, food packaging, defense & security, medical field, energy conversion and storage, environmental remediation, etc. [11-14].

As industrialization increases to accomplish the demands of the increasing population the natural environment becomes more and more contaminated with time. Industrialization is

compensating for the demands of the increasing population but on the other hand, dumping industrial waste into water, air, or land without processing is destroying the natural fresh environment. So, there is a need to produce materials and techniques to save the environment from being destroyed by these contaminants [15-17]. Nanoparticles created huge interest due to their very small size and large surface-to-volume ratio, and they display novel uniqueness in contrast to the large particles of bulk material [11-13]. The use of nanoparticles can overcome these problems due to the use of less quantity which makes them good adsorbents. Nanoparticles also served in photo catalyzed adsorption-degradation reactions for the removal of dyes and other organic contaminants [18, 19].

Silver nanoparticles can be synthesized by several physical, chemical, and biological methods. The biosynthesis methods have been replaced by chemical methods due to their eco-friendly nature can be used for the degradation of dye [20].

2. EXPERIMENTAL SECTION

2.1. Materials and Methods

The leaves of *Azadirachta Indica* were collected from Karachi, Pakistan. Silver nitrate ($AgNO_3$) (99.99%), Methyl violet, Sodium hydroxide (NaOH), and Hydrogen peroxide (H_2O_2), were procured from E. Merck.

2.2. Preparation of the Azadirachta Indica Leaf Extract

Leaves of *Azadirachta Indica* were washed and dried and cut into small pieces, the calculated amount of fresh leaves was boiled in deionized water 25-100(v/v) for 60 mins at room temperature and filtered.

2.3. Methyl Violet

N(4(dimethylamino)phenyl)methylene) cyclohexane-2,5-dien-1-ylidene) methane chloride commonly known as methyl violet heaving formula weight 393.96 g/mol, λ_{max} 583 nm used a stock solution of dye with conc. $1x10^{-5}$ $mol.dm^3$ was prepared in distilled water.

2.4. Syntesis of Silver Nanoparticles

Silver nanoparticles have been synthesized by adding 1 mL extract to preheated 50 mL, 1×10^{-4} mol/dm^3 silver nitrate solution and boiled at 323K for 2 min with continuous stirring. The formation of silver nanoparticles was indicated by the appearance of yellowish-brown color within 5 min. The nanoparticle solution underwent centrifugation at 12,000 rpm to separate nanoparticles. Afterward, a washing step removed impurities, and thorough drying ensured the purification of nanoparticles, yielding a refined sample.

2.5. Characterization of AgNPs

UV-vis spectrum, FTIR, and AFM, techniques were used for the characterization of AgNPs. UV-vis spectroscopic studies were carried out by (Shimadzu UV-160A, Japan, and Thermocouple Corporation, England). The FTIR spectra were recorded on wavelengths ranging from 500 cm^{-1} to 400 cm^{-1}. A scanning probe microscope used to create a topographical image of the sample is the Atomic Force Microscope.

2.6. Catalytic Degradation Assay

The catalytic activities of synthesized AgNPs were evaluated by degradation of methyl violet solution in the presence and absence of H_2O_2. A known volume (0.7, 1, and 1.3 ml) of silver nanopartwass was mixed with 1.5ml of methyl violet solution. The rate of the reaction was analyzed by observing the change of the absorption intensity at regular time intervals at 583nm. The percentage of degradation was calculated using the following equation.

$$\text{Decolorization\%} = (A_0 - A)/A_0 \times 100\%$$

2.7. Media Preparation for Antibacterial Activity

Weighed accurately 30.0 gm antibiotic Agar USP and transferred into 100 ml

distilled water. The media was autoclave at 394 K and pressured for about 15 mins.

2.8. Inoculum Preparation

The method of drilling holes was used to assay the antimicrobial activities of the AgNPs. Antibacterial activities were analyzed using S. Aurous ATTCC 6538, Bacillus Subtilis, and P. Aeruginosa ATTcc9027. The appropriate volume of the nanoparticle samples transfers to the fluid Thioglyconate medium (FTM). Antibacterial activity was measured using the Agar well method, the inhibition of different species. Isolate species from different techniques were placed on one side of the plate and the well was made through a cork borer. The well was poured with an NPs solution. The plates were incubated overnight at 310 K and antibacterial activity was measured.

3. RESULTS AND DISCUSSION

3.1. Characterization of AgNPs

3.1.1. UV-vis Spectroscopy

The UV-spectrum of methyl violet observed in H_2O showed from 200 to 800nm. The value of λ max and molar absorptivity coefficient (ϵ) of methyl violet obtained was found to be 583nm and $2.3x10^{-4}$ mol $^{-1}$ .dm ^{3} .cm $^{-1}$ respectively. The representative spectrum was shown in Figure 1a.

The formation of silver nanoparticles is observed by the color of the solution changing from yellow to dark brown after $AgNO_3$ solution was added to the extract of *Azadirachta Indica*, indicating the formation of AgNPs. The formation of AgNPs was further confirmed by recording UV-vis spectra and the maximum absorbance for AgNPs solution was detected at 400 nm as shown in Figure 1b.

3.1.2. Effect of pH on the Absorbance of Nanoparticles

The UV-vis spectra of AgNPs were taken at different pH in ranges from 2 to 11. The change in the acidity of the solution affected the absorption and the high value of absorbance was recorded in basic pH 11 which showed the formation of silver nanoparticles is favored in the basic medium. The UV-vis spectrum of silver nanoparticles at different pH is shown in Figure 2.

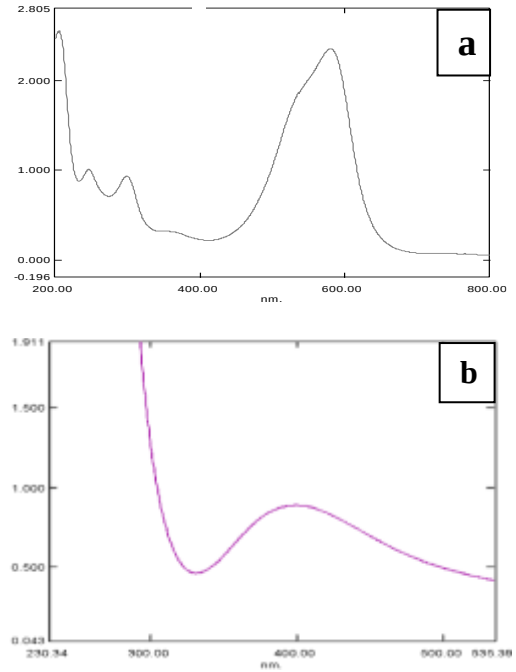

Figure1.(a) *Absorption spectrum of methyl violet of concentration $5x10^{-5}$ ($mol.dm^{-3}$) in aqueous medium.(b) Absorption spectrum of AgNPs in aqueous medium at pH 11.*

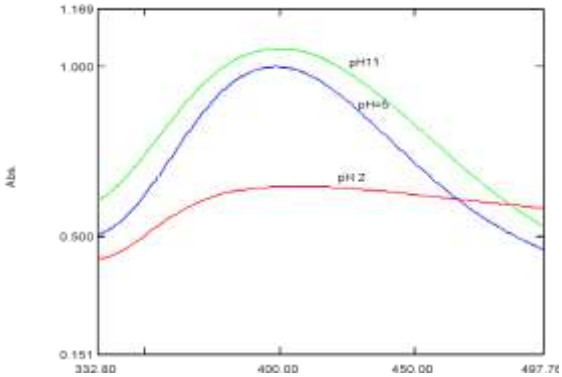

Figure 2. *Absorption spectrum of AgNPs at different pH.*

3.1.3. Fourier-Transform Infrared Spectroscopy

FTIR spectrum of *Azadirachta Indica* leaf extract and synthesized silver nanoparticles were analyzed. The role of the plant extract as a reducing and capping agent and the presence of some functional groups was confirmed by FTIR analysis of silver nanoparticles. The Broadband

between 3454.51 cm^{-1} is due to the O–H stretching vibration of group OH and the overlapping of the stretching vibration attributed to water and *Azadirachta indica* leaf extract molecules. The band at 1645 cm^{-1} corresponds to amide C=O stretching and a peek at 2069.62cm^{-1} can be assigned to the alkyne group. The observed peaks at 1130cm^{-1} denote –C–OC- linkages, or –C–O- bonds FTIR spectra of synthesized AgNPs are shown in Figure 3 respectively. From FT–IR results, it was concluded that some of the bio-organics compounds from *Azadirachta indica* extract formed a strong coating/capping on the nanoparticles. The results show the band that occurs at 607 cm^{-1} represents the formation of nanoparticles as shown in Figure 3.

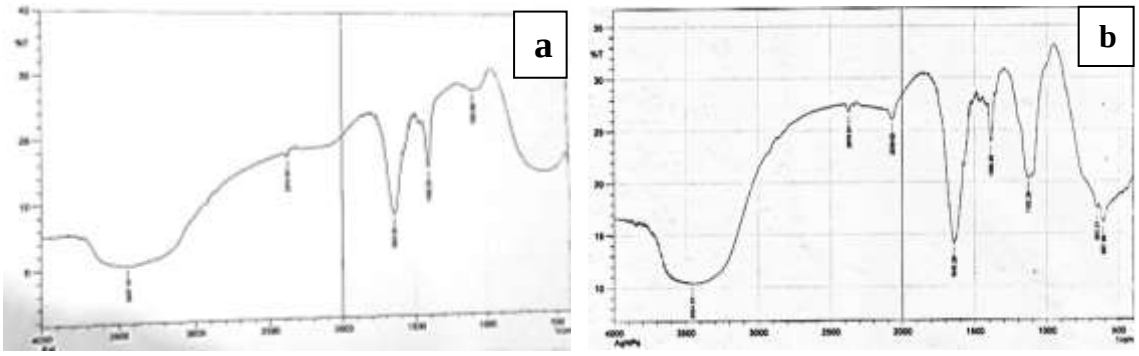

Figure 3. *FTIR spectra leaves of Azadirachta Indica spectra and synthesized AgNPs.*

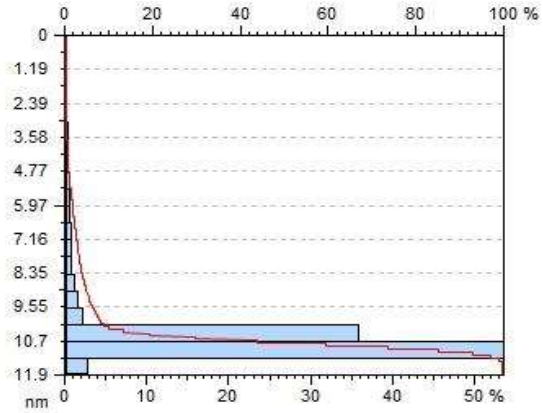

Figure 4. *Atomic force microscopy image of AgNPs.*

3.1.4 Atomic Force Microscopy (AFM)

Atomic Force Microscopy has been used to characterize AgNPs reduced in plant extract parts, to confirm their detail size, morphology, and agglomeration. it was evaluated that the biologically reduced AgNPs have a spherical shape in the range of 10 nm as observed by their topography on the surface, shown in Figures 4 and 5 respectively.

The AFM figure demonstrates that the nanoparticles exhibit sizes within the range of 10 nanometers.

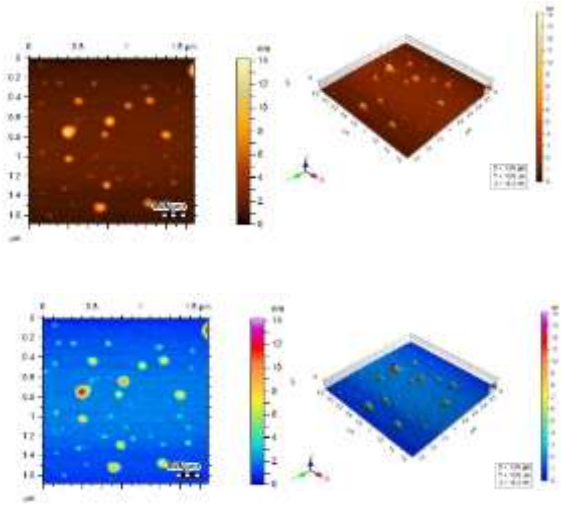

Figure 5. *Atomic force microscopy image of AgNPs.microscopy image of AgNPs.*

3.1.4. Zeta-Potential

Size and zeta-potential of AgNPs were investigated using Zetasizer Nano ZSP (Malvern). Average size of silver nanoparticles were found to be 95 nm as shown in Figure 6.

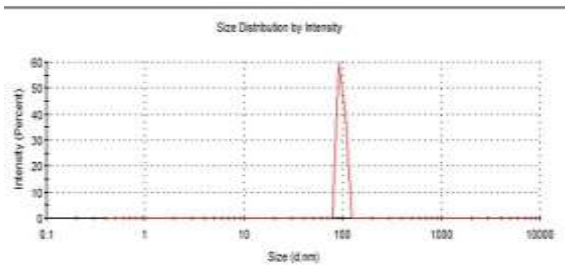

***Figure 6**. zeta-potential of AgNPs.*

3.2. Kinetics of Degradation

The kinetics of catalytic degradation of methyl violet using synthesized silver nanoparticles was studied at temperatures ranging between 298 K to 318 K at λ_{max} 583 nm. It was observed that absorbance decreased with respect to time with the increase in the concentration of AgNPs and the rate of the degradation of methyl violet with nanoparticles increased by the presence of H_2O_2 and the degradation time was reduced. The results showed that percent degradation increased with an increase in the concentration of AgNPs represented by the y pie chart shown in Figure 6. The rate degradation was high in presence of H_2O_2 and temperatureserature with maximum efficiency of 88.37%.

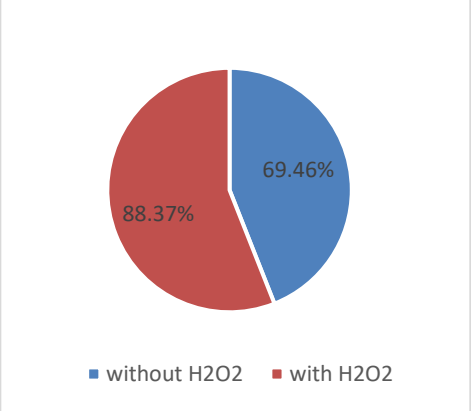

***Figure 6**. The absorbance of dye with AgNPs and in the presence of a catalyst.*

The degradation kinetics of methyl violet by AgNPs was also investigated in the absence and presence of H_2O_2 in the basic medium at pH 11. The results at different concentrations of nanoparticles and temperatures tabulated in table 1 showed that the % degradation increased with an increase in the concentration of AgNPs and H_2O_2 and decreased with a rising in temperature.

***Table 1.** Percentage degradation of silver nanoparticles at different temperatures.*

The volume of AgNPS ml	**298K**	**303K**	**308K**	**313k**	**318K**
0.7	66.39	66.17	57.03	46.6	20.02
1	73.11	72.62	73.57	55.54	47.19
H_2O_2					
0.7	88.37	76.35	84.79	83.23	80.64
1	77.19	75.48	84.39	82.59	78.41

The kinetic analysis of data showed that the plots of ln (At - A∞) with respect to time showed a linear relationship with R= 0.99 suggesting following pseudo-first-order kinetics. The rate constant for the degradation process influenced by the temperature is reported in table 2. The representative graph is shown in Figures 7 and 8.

It was observed that the rate constant decreased with an increase in temperature from 298K to 318 K.

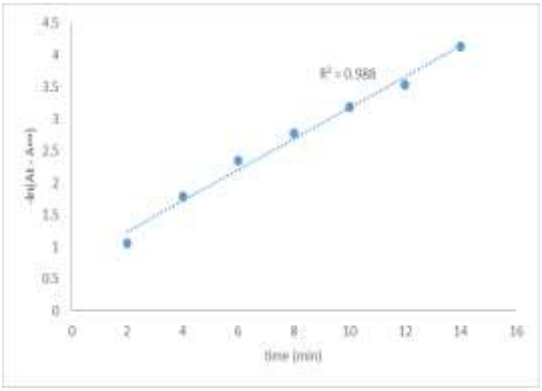

Figure 7*. Plot of ln(At - A∞) vs time for degradation of methyl violet with AgNPs (1.3ml) at 298K in the presence of a catalyst.*

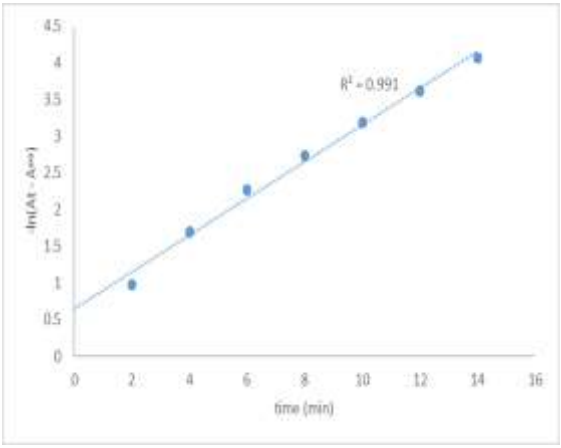

Figure 8*. Plot of ln(At - A∞) vs time for degradation of methyl violet with AgNPs (0.1ml) at 298K in the presence of a catalyst.*

The percent degradation of methyl violet was also observed high at 298K and low values were observed at high temperature showed that degradation is more favorable at low temperature.

Table 2. *Rate constant (k) for degradation of methyl violet with silver nanoparticles at different temperature.*

	Rate constant k_{obs}(min^{-1})	
Temp (k)	**0.7ml**	**1.0ml**
298	0.0676	0.0813
303	0.0634	0.0827
308	0.0602	0.0798
313	0.0392	0.0605
318	0.0469	0.0549
H_2O_2		
298	0.157	0.2732
303	0.3403	0.3367
308	0.3725	0.387
313	0.3975	0.4116
318	0.383	0.4239

Table 3. *Rate constant (k) for pseudo-first order and zero-order reactions at various temperatures (in Kelvin) for different volumes (0.7 ml and 1.0 ml).*

Temp (k)	**Pseudo-1st order**			
	0.7ml	R2	**1.0ml**	R2
298	0.068	0.988	0.081	0.991
303	0.063	0.996	0.083	0.987
308	0.06	0.989	0.08	0.989
313	0.039	0.987	0.061	0.99
318	0.047	0.984	0.055	0.994

Temp (k)	**zero-order**			
	0.7ml	**R2**	**1.0ml**	**R2**
298	0.0398	0.879	0.039	0.848
303	0.0435	0.939	0.037	0.79
308	0.0323	0.949	0.0409	0.766
313	0.027	0.9834	0.0331	0.919
318	0.016	0.976	0.0319	0.978

The variation in dye absorbance in the presence of silver nanoparticles over time was examined to investigate the kinetics of the process. The kinetic data was observed to conform well to a pseudo-first order relationship, as depicted in Table 3, with R-squared (R2) values of 0.99.

The mechanism of research was shown by kinetics study showed that presence of amino groups in the aromatic rings of methyl violet, along with its conjugated aromatic structure, influences its interaction with synthesized silver nanoparticles. These interactions facilitate the degradation process by enabling electron transfer, surface binding, and potentially initiating the breakdown of the dye molecule, making these functional

groups pivotal in the degradation mechanism.

3.3. Thermodynamic Parameter

The activation ion energy for degradation of methyl violet with synthesized AgNPs in an aqueous medium was determined using the Arrhenius equations.

$$\ln k = -Ea^*/RT + \ln A \quad (1)$$

where *k* is a rate constant, R is the general gas constant, T is absolute temperature, A is the Frequency factor and Ea* is the energy of activation. The activation energy was determined from the slope of the plot lnk versus 1/T.

Thermodynamic parameters including Gibbs free energy ΔG, change enthalpy ΔH, and change entropy ΔS are the parameters showing the temperature effect on the degradation of dye. The Change in enthalpy ΔH, standard entropy, ΔS, and ΔG were tabulated in table 3 by the relations:

$$\ln A = \ln (K_b T/h) x \Delta S/R \quad (2)$$

$$\Delta H = Ea - RT \quad (3)$$

$$\Delta G = \Delta H - T\,\Delta S \quad (4)$$

The value of activation energy (**Ea***), entropy change of activation (**ΔS**), enthalpy change of activation (**ΔH**), and Gibbs free energy change of activation (**ΔG**) are tabulated in Table 3.

Table 4. *Thermodynamic parameters of degradation of methyl violet.*

Activation parameters	AgNPs without catalyst	AgNPs with catalyst
Ea*(kJ.mol^{-1})	13.930	12.934
ΔH(kJ.mol^{-1})	11.453	10.467
ΔS(J.mol^{-1})	-2.339	1.14
ΔG(kJ.mol^{-1})	12.15	10.127

3.4. Antibacterial Assay

The antimicrobial sensitivity of AgNPs was tested on s. aurous ATTCC 6538, Bacillus Subtilis, and P. Aeruginosa ATTcc9027. For this purpose, the 20 mcg/ml and 4 mcg/ml concentration levels were prepared in water. The minimum inhibitory concentrations were assessed. The obtained MIC values have been tabulated in table 4. The antibacterial assy of AgNPs were shown in Figures 9 and 10.

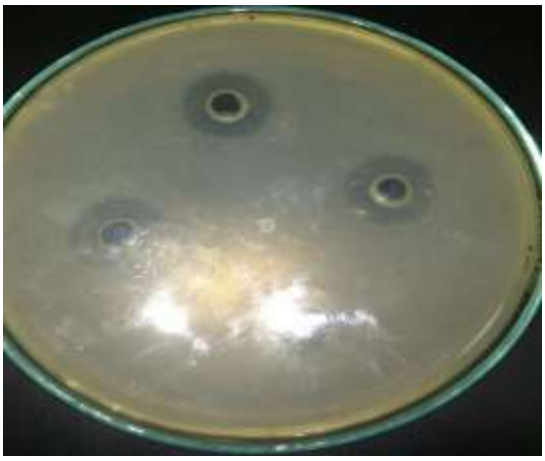

Figure9. *The antimicrobial activity of AgNPs at 20 mcg/ml of Bacillus Subtilis.*

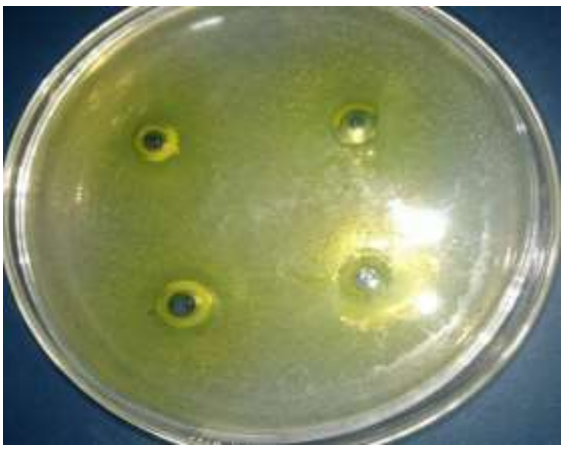

Figure 10. *The antimicrobial activity of AgNPs 4 mcg/ml of Bacillus Subtilis.*

Table 5. *Tra three constant (k) for degradation of methyl violet with silver nanoparticles at different temperature.*

S. No	Culture Type	Concentration (mcg)	Zone of Inhibition
1	S. Aurous	4.0	13
		20.0	24
2	Bacillus Subtilis	4.0	15
		20.0	25
3	P. Aeruginosa	4.0	12
		20.0	21

4. CONCLUSION

The kinetics of degradation of methyl violet with silver nanoparticles in the presence of a catalyst in an aqueous medium was studied spectrophotometrically. Aqueous extracts of leaves of Azadirachta indica were used for the synthesis of silver nanoparticles. The synthesized nanoparticles were identified and characteristics by spectrophotometer techniques. Absorption peaks from 300 to 400 nm in UV-Vis spectra showed the formation of nanoparticles, which were confirmed by metallic bond at 605 to 608 cm^{-1} in FTIR spectra. Atomic force microscopy (AFM) images confirm the spherical shape and size of nanoparticles and the high production of silver NPs. The reaction follows pseudo-first-order. Kinetics and rate of degradations of dye increased with an increase in the concentration of AgNPs, in presence of an H_2O_2 catalyst, and were favorable at low temperatures. Activation parameters also show the enhancement of reaction in presence of a catalyst. The antimicrobial activity of AgNPs against Bacillus Subtilis bacteria was found more efficient as compared to S. Aurous and P. Aeruginosa.

The degradation mechanism of methyl violet by AgNPs is multifaceted and influenced by various parameters. Concentration of AgNPs serves as a critical factor in augmenting degradation efficiency, while lower temperatures and the presence of H2O2 significantly accelerate the process. The findings strongly advocate for a combination of lower temperatures, elevated AgNP concentrations, and the addition of H2O2 to optimize the degradation efficiency of methyl violet. These findings hold promise for potential applications in environmental remediation processes, offering valuable insights for further research and practical implementation in pollution control and remediation strategies.

ACKNOWLEDGMENT

One of the authors (R.S) thanks the Dean Faculty of Science, University of Karachi, for the award of a research grant to carry out the present work.

CONFLICT OF INTEREST

The authors declare that they have no conflict of interest.

REFERENCES

1. Daneshvar, N., Ayazloo, M., Khataee, A. R., Pourhassan, M., "Biological decolorization of dye solution containing Malachite Green by microalgae Cosmarium sp.", *Bioresource Technology*, 98(6) (2007) 1176-1182.
2. Natarajan, S., Bajaj, H. C., Tayade, R. J., "Recent advances based on the synergetic effect of adsorption for removal of dyes from waste water using photocatalytic process", *Journal of Environmental Sciences*, 65 (2018) 201-222.
3. Zucca, P., Cocco, G., Sollai, F., Sanjust, E., "Fungal laccases as tools for biodegradation of industrial dyes", *Biocatalysis*, 1(1) (2016) 82-108.
4. Entwistle, C. D., Marder, T. B., "Applications of three-coordinate organoboron compounds and polymers in optoelectronics", *Chemistry of Materials*, 16(23) (2004) 4574-4585.
5. Dong, M., Babalhavaeji, A., Samanta, S., Beharry, A. A., Woolley, G. A., "Red-shifting azobenzene photoswitches for in vivo use", *Accounts of Chemical Research*, 48(10) (2015) 2662-2670.
6. Stromberg, J. R., Marton, A., Kee, H. L., Kirmaier, C., Diers, J. R., Muthiah, C., Taniguchi, M., Lindsey, J. S., Bocian, D. F., Meyer, G. J., Holten, D., "Examination of tethered porphyrin, chlorin, and bacteriochlorin molecules in mesoporous metal-oxide solar cells", *The Journal of Physical Chemistry C*, 111(42) (2007) 15464-15478.
7. Chequer, F. D., De Oliveira, G. R., Ferraz, E. A., Cardoso, J. C., Zanoni, M. B., De Oliveira, D. P., "Textile dyes: dyeing process and environmental impact", *Eco-friendly textile dyeing and finishing*, 6(6) (2013) 151-176.
8. Jani, M. M., "*Studies on intrinsic microbial populations of contaminated environment and biodegradative potentials",* Doctoral dissertation, Saurashtra University.
9. Duxbury, D. F., "The sensitized fading of triphenylmethane dyes in polymer films: Part 1", *Dyes and pigments*, 25(2) (1994) 131-166.

10. Shindhal, T., Rakholiya, P., Varjani, S., Pandey, A., "Ngo HH, Guo W, Ng HY, Taherzadeh MJ. A critical review on advances in the practices and perspectives for the treatment of dye industry wastewater", *Bioengineered*, 12(1) (2021) 70-87.
11. Kim, B. H., Hackett, M. J., Park, J., Hyeon, T., "Synthesis, characterization, and application of ultrasmall nanoparticles", *Chemistry of Materials*, 26(1) (2014) 59-71.
12. Scheu, M., Veefkind, V., Verbandt, Y., Galan, E. M., Absalom, R., Förster, W., "Mapping nanotechnology patents: The EPO approach", *World Patent Information*, 28(3) (2006) 204-211.
13. Mittal, J., Batra, A., Singh, A., Sharma, M. M., "Phytofabrication of nanoparticles through plant as nanofactories", *Advances in Natural Sciences: Nanoscience and Nanotechnology*, 5(4) (2014) 043002.
14. Kumari, M. M., Ananthalakshmi, R., Indo–Asian Journal of Multidisciplinary Research (IAJMR).
15. Eneh, O. C., "Managing Nigeria's environment: The unresolved issues", *Journal of Environmental Science and Technology*, 4(3) (2011) 250-263.
16. Pereira, L., Alves, M., "*Dyes-environmental impact and remediation in environmental protection strategies for sustainable development*", Springer, Dordrecht, (2012).
17. Ali, H., "Biodegradation of synthetic dyes-a review", *Water, Air, & Soil Pollution*, 213(1) (2010) 251-273.
18. Liu, Y., Jin, W., Zhao, Y., Zhang, G., Zhang, W., "Enhanced catalytic degradation of methylene blue by α-Fe2O3/graphene oxide via heterogeneous photo-Fenton reactions", *Applied Catalysis B: Environmental*, 206 (2017) 642-652.
19. Tyagi, S., Rawtani, D., Khatri, N., Tharmavaram, M., "Strategies for nitrate removal from aqueous environment using nanotechnology: a review", *Journal of Water Process Engineering*, 21 (2018) 84-95.
20. Vasantharaj, S., Sathiyavimal, S., Saravanan, M., Senthilkumar, P., Gnanasekaran, K., Shanmugavel, M., Pugazhendhi, A., "Synthesis of ecofriendly copper oxide nanoparticles for fabrication over textile fabrics: characterization of antibacterial activity and dye degradation potential", *Journal of Photochemistry and Photobiology B: Biology*, 191 (2019) 143-149.